REPORT

Homozygous Mutations in Fibroblast Growth Factor 3 Are Associated with a New Form of Syndromic Deafness Characterized by Inner Ear Agenesis, Microtia, and Microdontia

Mustafa Tekin, Burcu Öztürk Hişmi, Suat Fitoz, Hilal Özdağ, Filiz Başak Cengiz, Aslı Sırmacı, İdil Aslan, Bora İnceoğlu, E. Berrin Yüksel-Konuk, Seda Taşır Yılmaz, Öztan Yasun, and Nejat Akar

We identified nine individuals from three unrelated Turkish families with a unique autosomal recessive syndrome characterized by type I microtia, microdontia, and profound congenital deafness associated with a complete absence of inner ear structures (Michel aplasia). We later demonstrated three different homozygous mutations (p.S156P, p.R104X, and p.V206SfsX117) in the fibroblast growth factor 3 (*FGF3*) gene in affected members of these families, cosegregating with the autosomal recessive transmission as a completely penetrant phenotype. These findings demonstrate the involvement of *FGF3* mutations in a human malformation syndrome for the first time and contribute to our understanding of the role this gene plays in embryonic development. Of particular interest is that the development of the inner ear is completely disturbed at a very early stage—or the otic vesicle is not induced at all—in all of the affected individuals who carried two mutant *FGF3* alleles.

The incidence of congenital sensorineural hearing loss in developed countries is 1.33–1.86 per 1,000 newborns.[1] Radiological abnormalities of the inner ear are detected in ~30% of these children.[2,3] Complete bony and membranous aplasia of the inner ear, which was first described by Michel in 1863[4] and is referred to as "Michel aplasia," is among the rare examples of inner ear anomalies. Deafness, sometimes associated with inner ear anomalies, is a phenotypic component of >400 multiple-malformation syndromes. We have delineated a new autosomal recessively inherited human malformation syndrome in three unrelated Turkish families including nine affected individuals ranging in age from 7 to 42 years (figs. 1 and 2). Three major phenotypic effects noted in all affected individuals were profound congenital sensorineural deafness, type I microtia with shortening of auricles above the crura of antihelix, and microdontia with widely spaced teeth. In addition, anteverted ears were present in seven of the nine affected individuals (fig. 2). Computed tomography (CT) of the temporal bones in all patients showed the complete absence of inner ear structures bilaterally, including cochlea, vestibule, and semicircular canals (Michel aplasia) with normal-appearing middle ear structures (figs. 3 and 4). In addition to CT examination, a cranial magnetic resonance imaging of the cerebellopontine angle showed the bilateral absence of cochleovestibular nerve with otherwise normal cerebral and cerebellar structures in one affected patient (fig. 5). Physical development was normal in all patients. The standing heights of two patients were above the 97th percentile for normal Turkish children at the same ages. A delay in gross motor skills during infancy, presumably caused by impaired balance, was noted in all patients. Seven affected subjects were students at local schools for the hearing impaired and had no difficulties in writing or reading. All children were reported to be average or above average students, with no problems communicating by use of an indigenous sign language. Individual III:3 in family B had a paying job and was responsible for the support of his family. Therefore, the affected subjects appeared to have normal cognitive abilities. Complete blood counts, serum electrolytes, and results of liver and kidney function tests were all within normal limits, and the lacrimal canals and saliva production were normal. There were no limb anomalies on clinical examination or on X-rays. Renal ultrasound in one girl (family A, IV:10) showed unilateral stenosis of ureteropelvic junction. Another girl (family C, II:1) was operated on for strabismus at a young age and wore glasses for hypermetropia. Ophthalmoscopic evaluation of all cases showed normal retinal findings. A supernumerary upper lateral incisor was present, with absence of the first premolar on the same side in one person (family A, IV:5). Some affected individuals had peg-shaped lateral incisors and loss of tooth heights because of physical contact between the upper and lower teeth. Mild micrognathia was noted in some patients. Excessive caries were noted only in the 42-year-old male (family B, III:3), probably reflecting poor oral hygiene (fig. 2). Peripheral blood chromosomes were normal in one patient from each family. None of the parents had any of the above-mentioned clinical findings. The presence of auriculodental

From the Division of Clinical Molecular Pathology and Genetics, Department of Pediatrics (M.T.; B.Ö.H.; H.Ö.; F.B.C.; A.S.; İ.A.; B.İ.; E.B.Y-K.; N.A.) and Department of Radiodiagnostics (S.F.), Ankara University School of Medicine; Biotechnology Institute of Ankara University (H.Ö.; S.T.Y.); and Department of Dentistry, Ankara Numune Hospital (Ö.Y.), Ankara, Turkey

Received October 6, 2006; accepted for publication November 15, 2006; electronically published December 27, 2006.

Address for correspondence and reprints: Dr. Mustafa Tekin, Birlik Mah 65.Sok No:20/7, Çankaya, Ankara, 06610, Turkey. E-mail: mtekin@medicine.ankara.edu.tr

Am. J. Hum. Genet. 2007;80:338–344. 0002-9297/2007/8002-0013$15.00

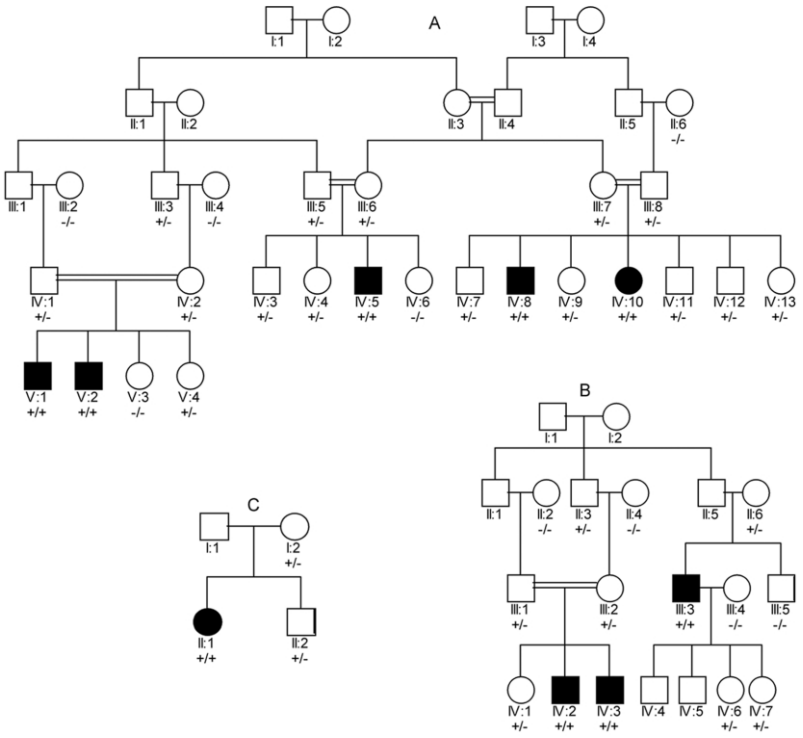

Figure 1. Pedigrees of three unrelated Turkish families with the syndrome described in this report. Plus and minus signs indicate the presence and absence of the identified mutation, respectively. Mutations were c.466T→C, c.310C→T, and c.616delG, in families A, B, and C, respectively. Although consanguinity was denied between I:1 and I:2 in family C and between II:5 and II:6 in family B, parents originated from a small, isolated village in both families. Consanguinity between II:3 and II:4 in family A is more distant than third-degree cousins.

findings was somewhat suggestive of the lacrimoauriculodentodigital (LADD) syndrome (MIM 149730). However, the lacrimal and digital findings and dominant transmission of LADD[5] were absent in our patients, who clearly showed autosomal recessive inheritance. A search of OMIM and POSSUM with the keywords "microtia," "deafness," "absence of inner ear," "Michel aplasia," and "microdontia" did not match other recognized syndromes. A report of a sporadic case with Michel aplasia, microdontia, and microtia was noted during a search in PubMed.[6] We concluded that the phenotypic findings described in our patients and in the child previously reported by Hersh et al.[6] represent a distinct autosomal recessive multiple-malformation syndrome.

After obtaining written informed consent using forms approved by the Ankara University Ethics Committee (decision no. 85–2215; January 30, 2006), we obtained DNA samples from available family members. Genomic DNA was extracted from peripheral blood by a standard phenol chloroform method. Because of the phenotypic similarities between LADD syndrome and the new syndrome, we initially suspected that a homozygous mutation involving a member of the fibroblast growth factor family might be responsible. To find such a candidate gene, we genotyped 19 members of family A for 10,200 SNPs with a mean intermarker distance of 258 kb, equivalent to 0.36 cM, using Affymetrix GeneChip 10K Xba 142 2.0. The recommendations by Affymetrix were followed throughout the study. Experiments were performed at the Central Genomics Laboratory of Ankara University Biotechnology Institute. For linkage analysis, the SuperLink v1.4 and GeneHunter v2.1r5 programs were used in the easyLINKAGE Plus v4.01 beta program package written for Windows.[7] An autosomal recessive inheritance model with full penetrance was selected. Frequency of the disease allele was 0.001. Affymetrix Marshfield SNP data were used for mapping information of the genotyped SNPs. Raw data obtained from GeneChip were converted to a Microsoft Excel table, and linkage analysis was performed on a personal computer located at the Division of Clinical Molecular Pathology and Genetics of Ankara University. These analyses did not provide a significant LOD score for any tested marker (fig. 6). Because the family contained consanguineous marriages, we looked for homozygous SNP blocks that were shared by all affected subjects. This approach, although empirical, has been shown to be effective for identifying regions of identity by descent (IBD) during the evaluation of genomewide SNP data.[8,9] It has been shown that the greater the number of affected individuals who have a shared homozygous region and the greater the size

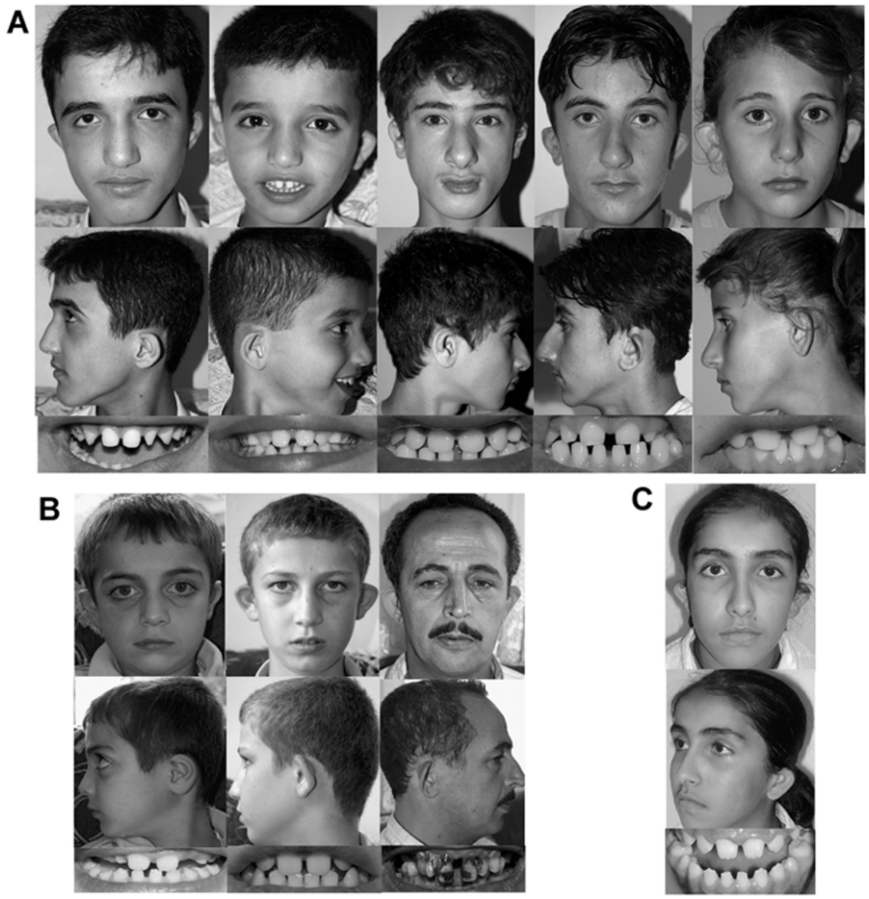

Figure 2. Clinical photographs of the affected nine subjects. Note the presence of type I microtia and microdontia in all patients. A long face was seen in most affected subjects, growing more pronounced as they got older. *A,* From left to right, V:1, V:2, IV:5, IV:8, and IV:10 in family A. *B,* IV:3, IV:2, and III:3 in family B. *C,* II:1 in family C. The hearing members of the families have normal-appearing teeth and no craniofacial dysmorphology.

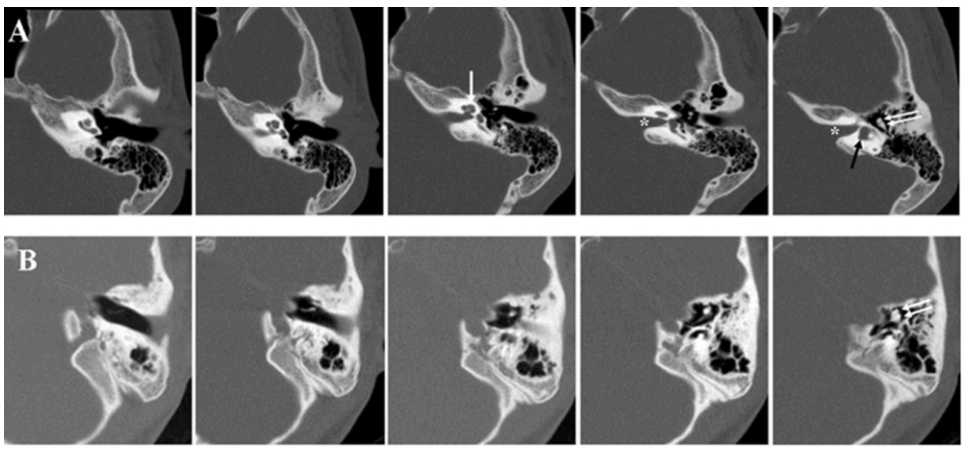

Figure 3. *A,* Contiguous axial CT sections of normal temporal bone. Cochlea (*white arrow*), internal auditory canal (*asterisk*), vestibule (*black arrow*), and ossicles (*double white arrows*) are clearly visible. *B,* CT images crossing through approximately the same levels, compared with normal sections, reveal petrous bone aplasia, with absence of inner ear structures in II:1 in family C. Normal development of middle ear cavity and ossicles (*double arrow*) are clearly visible. CT images in all affected subjects showed similar findings (fig. 4).

The figure is available in its entirety in the online edition of *The American Journal of Human Genetics*.

Figure 4. Contiguous axial CT sections of normal temporal bone. The legend is available in its entirety in the online edition of *The American Journal of Human Genetics*.

of the region, the more likely the region is to harbor the mutation that causes the disease.[8,9] Because the exclusion of a given locus was based on its heterozygosity, we included all SNPs in the analysis without taking into account their informativeness or "no call" genotypes. Visual evaluation of our data showed that all five affected individuals in family A were homozygous for nine consecutive SNPs between *rs1944043* and *rs2077955,* corresponding to a physical position of 62,620,442–71,886,708 bp or a span of 9,266,266 bp (table 1), implying but not confirming IBD for this locus. The genomic localization of *FGF3* (Ensembl accession number ENSG00000186895) is between 69,333,917 and 69,343,129 bp on 11q13. Because we previously hypothesized that a fibroblast growth factor was involved in the pathogenesis of this syndrome and *FGF3* has previously been shown to be expressed during inner ear and tooth development,[10] we considered this gene to be a prime positional candidate instead of documenting a formal linkage by use of genotypes of a greater number of polymorphic markers. The three exons and intron-exon boundaries of the *FGF3* gene were PCR amplified using specific primers designed with the Primer3 program (table 2). PCRs were performed in a total volume of 50 μl containing 100 ng genomic DNA, 20 pmol each primer, 200 μM deoxynucleotide triphosphates, 1 U thermostable DNA polymerase (Fermentas), and 1.5 mM $MgCl_2$. Betaine was added to increase the product yield in some reactions. The PCR products were later purified using a DNA clean and concentrator-5 kit (Zymo Research) and sequenced in both directions using a dye terminator cycle sequencing kit (Beckman Coulter) in all members of three families. An automated sequencer (Beckman Coulter CEQ 2000XL) was used for DNA sequencing.

We identified a homozygous c.466T→C mutation in the third exon of *FGF3* in five affected members of family A (fig. 7). All parents were heterozygous, and unaffected relatives were heterozygous or homozygous for the wild-type allele (fig. 1). This mutation substitutes an uncharged polar side chain amino acid, serine, with a nonpolar side chain residue, proline, at codon 156 of the *FGF3* protein (p.S156P). Proline residues are known to introduce kinks into the secondary protein structure. Serine at codon 156 is highly conserved during evolution (fig. 8). When we repeated linkage analysis using genotypes obtained for the c.466T→C mutation in the same 19 members of family A, we found a two-point parametric LOD score of 3.86 at a recombination fraction (θ) of 0. (When we included additional members of this family, who became available later, the LOD score was found to be 4.52 at $\theta = 0$).

We found a nonsense homozygous mutation, c.310C→T (p.R104X), in the second exon of *FGF3* in all three of the affected members of family B (fig. 7). All available parents were heterozygous, and unaffected relatives were heterozygous or homozygous for the wild-type allele in this family (fig. 1). This mutation presumably truncates more than one-half of the protein, apparently leaving behind a nonfunctional product. Finally, in the proband of family C, we found a homozygous c.616delG (p.V206SfsX117) mutation in the third exon of *FGF3* (fig. 7). The mother and a healthy brother were found to be heterozygous for this deletion (fig. 1). The mutation causes a frameshift starting

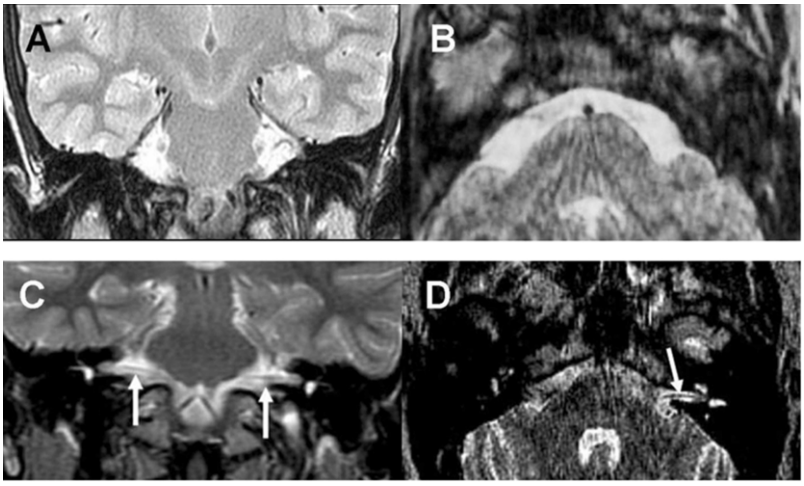

Figure 5. In a patient (family C, II:1) with bilateral inner ear petrous bone aplasia and absence of inner ear structures detected on CT (row B in fig. 3), coronal (*A*) and axial (*B*) MR images clearly show the absence of the internal auditory canal in cerebellopontine angle compared with normal appearances (*C* and *D*). *White arrows,* cochleovestibular nerves.

The figure is available in its entirety in the online edition of *The American Journal of Human Genetics*.

Figure 6. Graphical representation of the analysis of family A. The legend is available in its entirety in the online edition of *The American Journal of Human Genetics*.

from codon 206, resulting in the production of a completely altered protein that terminates after 116 codons.

All three mutations are likely to have significant effects on the resulting polypeptides and most likely result in nonfunctional proteins. The identified three mutations were screened using PCR–Single Strand Conformational Polymorphism (SSCP) or Amplification Refractory Mutation Detection System (ARMS) protocols in 300 healthy unrelated Turkish subjects (600 chromosomes). Primers of *FGF3* exon 2, 466sscp, 616delG, 466arms, and 310arms were used during PCRs (table 2). In SSCP, the PCR products were denatured at 94°C, loaded onto 7% nondenaturing polyacrylamide gels, run overnight at +4°C in a vertical gel electrophoresis system (DCode Universal Mutation detection System [BioRad]), and visualized with silver staining. Homozygous and heterozygous samples were loaded on each gel after confirmation of their differing band structures. Concentration of $MgCl_2$ was reduced to 1 mM to increase specificity of ARMS reactions. PCR products were loaded on 3% agarose gels and visualized under UV light. Homozygous and heterozygous controls were studied as positive controls in each PCR. All experiments were performed at the laboratories of the Clinical Molecular Pathology and Genetics Division in the Department of Pediatrics of Ankara University School of Medicine. None of the samples was found to be positive for anyone of the three screened mutations.

In the mouse, *Fgf3* mRNA has been detected in the hindbrain rhombemeres 5 and 6, adjacent to the otocysts, as well as in the pharyngeal pouches.[11] In studies of older embryos and newborn pups, *Fgf3* expression was detected in the developing cerebellum, retina, teeth, and inner ear.[11] The auricle develops from six auricular hillocks arising on the opposed surfaces of the first and second pharyngeal arches. The upper part of the auricle is derived from the dorsal part of the first pharyngeal arch. Our study suggests that the embryonic development of this area is dependent on FGF3 signaling in humans. Early development of the tooth appears not to be significantly affected in homozygotes. However, the diameters of almost all teeth were reduced, probably because of impaired FGF3 signaling for growth promotion. Recent findings of heterozygous loss-of-function mutations in genes coding Fgf-signaling proteins, *FGF10, FGFR2,* and *FGFR3,* in LADD[12,13] support the idea that Fgf signaling is crucial for normal auricle and tooth formation. Interestingly, reports of two previous mouse knockout models of *Fgf3* did not mention any disturbance of the external ears or tooth development.[14,15]

It is surprising to observe complete absence of inner ear structures in homozygous *FGF3* mutants in the human. The inner ear develops from the otic vesicle, which itself is formed by the invagination of a lateral thickening (placode) of the cephalic ectoderm of the vertebrate embryo, adjacent to hindbrain, at the level of rhombomeres 5 and 6. *Fgf3* is expressed in the developing hindbrain and has been shown to be involved in the inner ear development of a variety of vertebrates, including zebrafish, *Xenopus,* chick, and mouse. Treatment of chick hindbrain cultures containing otic placodes with reagents targeted against human FGF3 prevented the formation of otic vesicles.[16] It was also found that the ectopic expression of *Fgf3* results in the formation of ectopic otic vesicles and development of normal inner ear structures in avian embryos.[17] Despite these reports, the phenotypes of two murine *Fgf3* knockouts strongly argue against an essential role of *Fgf3* during

Table 1. Partial Results of 10K GeneChip Array in Family A, Showing the Chromosomal Region Containing *FGF3* (q13 Band of Chromosome 11)

dbSNP RS ID	Physical Position (bp)	Genotype in																			
		Affected Subjects					Unaffected Siblings								Parents						
		V:1	V:2	IV:8	IV:10	IV:5	V:3	V:4	IV:4	IV:6	IV:7	IV:11	IV:12	IV:13	III:5	III:6	III:7	III:8	IV:2	III:2	
rs953894	62518998	AA	AA	AA	AB	AA	AA	AB	AA	AA	AB	AA	AA	AA	AA	AA	AB	AA	AB	AB	
rs1944043	62620442	AA	AA	AA	AA	AA	AB	AA	AA	AA	AA	AA	AB	AB	AA	AA	AA	AB	AA	AA	
rs1944042	62620580	BB	BB	BB	BB	BB	AB	BB	BB	BB	BB	BB	AB	AB	BB	BB	BB	AB	BB	BB	
rs1944086	62793443	BB	00	00	BB	BB	AB	00	BB	AB	BB	00	AB	AB	AB	BB	00	AB	BB	AB	
rs1404501	63041086	BB	BB	BB	BB	BB	BB	BB	BB	BB	BB	BB	BB	BB	BB	BB	BB	BB	BB	BB	
rs490192	64227945	AA	AA	AA	AA	AA	AA	AA	AA	AA	AA	AA	AA	AA	AA	AA	AA	AA	AA	AB	
rs1938684	68986287	BB	BB	BB	BB	BB	AB	BB	BB	AA	AB	AB	AB	AB	AB	AB	AB	AB	BB	AA	
rs1944130	69291704	AA	AA	AA	AA	AA	AA	AA	AA	AA	AA	AA	AA	AA	AA	AA	AA	AA	AA	AA	
FGF3 c.466	69342539	CC	CC	CC	CC	CC	TT	TC	TC	TT	TC	TC	TC	TC	TC	TC	TC	TC	TC	TT	
rs1372108	70642724	AA	AA	AA	AA	AA	00	AA	AA	AA	AA	AA	AB	AB	AA	AA	AA	AB	AA	AA	
rs2077955	71886708	BB	BB	BB	BB	BB	BB	BB	BB	BB	BB	BB	BB	BB	BB	BB	BB	BB	BB	00	
rs1279293	73727821	BB	BB	BB	BB	AB	BB	BB	AB	AA	BB	BB	BB	BB	AB	AB	BB	BB	BB	AB	

NOTE.—All genotypes are shown as they appeared in the raw data obtained from the microarray system. Homozygous genotypes in five affected subjects are manually highlighted, and the results of mutation screening for c.466T→C in *FGF3* were later incorporated. Haplotypes created using these data are shown in figure 6.

Table 2. Primers and PCR Conditions Used

Gene	Primer		Annealing Temperature (°C)	Product Size (bp)
	Forward	Reverse		
FGF3:				
Exon 1	5′AGCACCTCGCAGCTGTCC-3′	5′GAGGCAGACGGTCTTTTCC-3′	57	476
Exon2	5′-GGAGTGAGGCACCTCTCATT-3′	5′-CCCTTGGCAAAGCATTCTAC-3′	60	237
Exon3	5′-CTGACGCTGCCACAGTCTC-3′	5′-CCAAGATGTCGCCAGGAG-3′	55	493
466sscp	5′-ATCCACGAGCTGGGCTATAA-3′	5′-CAGGGAGGACTTCTGTGTGC-3′	58	171
616delG	5′-CAGAAGTCCTCCCTGTTCCT-3′	5′-AGTCTCGAAGCCTGAACGTG-3′	58	173
466arms_mutant	5′-CCGAGAGACTGTGGTACGTGC-3′	5′-GCAGCCCACTCTGTAGCTG-3′	61	150
466arms_normal	5′-CCGAGAGACTGTGGTACGTGT-3′	5′-GCAGCCCACTCTGTAGCTG-3′	60	150
310arms_mutant	5′-GCCATGAACAAGAGGGGAT-3′	5′- CGGAGCAGCCTCTAACAGAC-3′	60	223
310arms_normal	5′-GCCATGAACAAGAGGGGAC-3′	5′- CGGAGCAGCCTCTAACAGAC-3′	60	223
FGF8:				
Exon 3	5′-TACTTAAAAGCGCCCTGCTC-3′	5′-CAGCCCAGGATGAACGAG-3′	62	154
Exon 4	5′-GGTGTATTGTGTATTTTTCAATTTCC-3′	5′-TCCCACAAGCTACCTTCAGC-3′	58	241
Exon 5	5′-CTTTGGAGCAGTTGCTGCTGG-3′	5′-AGCCCAGGACTGTCTTGGAGG-3′	60	283
Exon 6	5′-CCATGTGTCACTGCTGCCTGG-3′	5′-GGTGCCCTACAGGATGAGCC-3′	62	563
FGF10:				
Exon 1	5′-TGCCTTGCATCGGTTCTTACC-3′	5′-ATTTAGCTGGCCACATCTGG-3′	60	493
Exon 2	5′-TTGCTGGAAATACTTGCCGGG-3′	5′-AAGCTATCCGGTGTCTGGAGG-3′	60	383
Exon 3	5′-CAAACAGAATCCTTGGACTGG-3′	5′-CTTGGCAAAAGAGCCATTGG-3′	60	348

induction of the otic vesicle. In the first reported knockout model, some of the homozygous mutants had normal hearing but the majority developed hearing loss from inner ear anomalies related to the improper formation of the endolymphatic sac and duct.[14] Another mutant lacking the entire *Fgf3* coding region showed no evidence for severe defects either during inner ear development or in the mature sensory organ, suggesting the functional involvement of other Fgf family members during its formation.[15] Recent experiments in the mouse have documented the involvement of *Fgf10* and *Fgf8* in inner ear induction and early development, showing that double null mutants of *Fgf3* and *Fgf10* or *Fgf8* result in complete agenesis of the otic vesicles.[18,19] Because of the inconsistent phenotypes observed in the mouse knockouts and the remarkably consistent effects observed in our three families, we explored the possible involvement of other FGF genes in the pathogenesis of this new syndrome. Sequencing of the exons of human *FGF8* and *FGF10* genes in one affected subject from each family failed to reveal any sequence alterations (table 2). The monogenic autosomal recessive segregation of three *FGF3* mutations in our families thus makes the involvement of other genes unlikely. We conclude that FGF3 signaling is necessary for the early de-

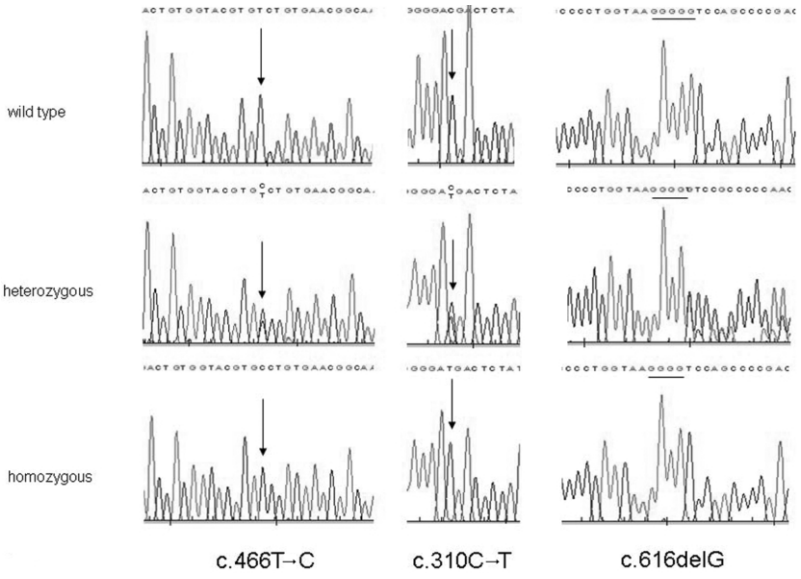

Figure 7. The c.466T→C (p.S156P), c.310C→T (p.R104X), and c.616delG (p.V206SfsX117) mutations. Arrows and lines indicate the mutation points.

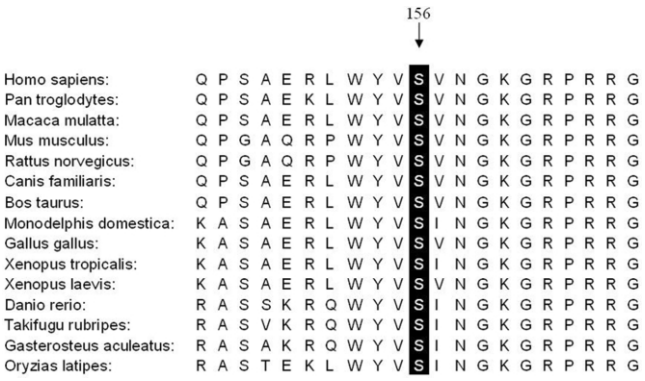

Figure 8. Serine at position 156 of *Fgf3* is conserved in a variety of organisms from fish to frogs to humans. Data were obtained using protein-protein BLAST at the National Center for Biotechnology Information Web site.

velopment of the inner ear in humans and, on the basis of the previous studies described above, that this requirement differs from the mouse.

Acknowledgments

This study was supported by the Turkish Research and Technology Council (TUBITAK) (grant no. SBAG-3271 to M.T.) and by funds from the Ankara University Biotechnology Institute. We thank Dr. Walter Nance from Virginia Commonwealth University for his careful review of the manuscript and helpful suggestions. We are grateful to Dr. Susan Blanton from Duke University for her review of our data before publication.

Web Resources

Accession numbers and URLs for data presented herein are as follows:

Ensembl database, http://www.ensembl.org/Homo_sapiens/index.html (for *FGF3* [accession number ENSG00000186895])
Online Mendelian Inheritance in Man (OMIM), http://www.ncbi.nlm.nih.gov/Omim/ (for LADD syndrome)
Primer3, http://frodo.wi.mit.edu/cgi-bin/primer3/primer3_www.cgi
Protein-protein BLAST, http://www.ncbi.nlm.nih.gov/blast/Blast.cgi

References

1. Morton CC, Nance WE (2006) Newborn hearing screening—a silent revolution. N Engl J Med 354:2151–2164
2. Bamiou DE, Phelps P, Sirimanna T (2000) Temporal bone computed tomography findings in bilateral sensorineural hearing loss. Arch Dis Child 82:257–260
3. Mafong DD, Shin EJ, Lalwani AK (2002) Use of laboratory evaluation and radiologic imaging in the diagnostic evaluation of children with sensorineural hearing loss. Laryngoscope 112:1–7
4. Michel P (1863) Memoire sur les anomalies congenitales de poreille intern. Gazette Med de Strasburg 23:55–58
5. Allanson J (2004) Genetic hearing loss associated with external ear abnormalities. In: Toriello HV, Reardon W, Gorlin RJ (eds) Hereditary hearing loss and its syndromes. Oxford University Press, Oxford, pp 101–102
6. Hersh JH, Ganzel TM, Fellows RA (1991) Michel's anomaly, type I microtia and microdontia. Ear Nose Throat J 70:155–157
7. Linder TH, Hoffmann K (2005) easyLINKAGE: A PERL script for easy and automated two-/multipoint linkage analyses. Bioinformatics 21:405
8. Woods CG, Valente EM, Bond J, Roberts E (2004) A new method for autozygosity mapping using single nucleotide polymorphisms (SNPs) and EXCLUDEAR. J Med Genet 41: e101
9. Carr IM, Flintoff KJ, Taylor GR, Markham AF, Bonthron DT (2006) Interactive visual analysis of SNP data for rapid autozygosity mapping in consanguineous families. Hum Mutat 27:1041–1046
10. Wilkinson DG, Bhatt S, McMahon AP (1989) Expression pattern of the FGF-related proto-oncogene int-2 suggests multiple roles in fetal development. Development 105:131–136
11. Wilkinson DG, Peters G, Dickson C, McMahon AP (1988) Expression of the FGF-related proto-oncogene int-2 during gastrulation and neurulation in the mouse. EMBO J 7:691–695
12. Milunsky JM, Maher TA, Colby R, Everman DB (2006) LADD syndrome is caused by FGF10 mutations. Clin Genet 69:349–354
13. Rohmann E, Brunner HG, Kayserili H, Uyguner O, Nurnberg G, Lew ED, Dobbie A, Eswarakumar VP, Uzumcu A, Ulubil-Emeroglu M, et al (2006) Mutations in different components of FGF signaling in LADD syndrome. Nat Genet 38:414–417
14. Mansour SL, Goddard JM, Capecchi MR (1993) Mice homozygous for a targeted disruption of the proto-oncogene int-2 have developmental defects in the tail and inner ear. Development 117:13–28
15. Alvarez Y, Alonso MT, Vendrell V, Zelarayan LC, Chamero P, Theil T, Bosl MR, Kato S, Maconochie M, Riethmacher D, et al (2003) Requirements for FGF3 and FGF10 during inner ear formation. Development 130:6330–6338
16. Represa J, Leon Y, Miner C, Giraldez F (1991) The int-2 proto-oncogene is responsible for induction of the inner ear. Nature 353:561–563
17. Vendrell V, Carnicero E, Giraldez F, Alonso MT, Schimmang T (2000) Induction of inner ear fate by FGF3. Development 127:2011–2019
18. Wright TJ, Mansour SL (2003) Fgf3 and Fgf10 are required for mouse otic placode induction. Development 130:3379–3390
19. Ladher RK, Wright TJ, Moon AM, Mansour SL, Schoenwolf GC (2005) FGF8 initiates inner ear induction in chick and mouse. Genes Dev 19:603–613